



Faculty of Manufacturing Engineering



Farah Hanum binti Suzaim

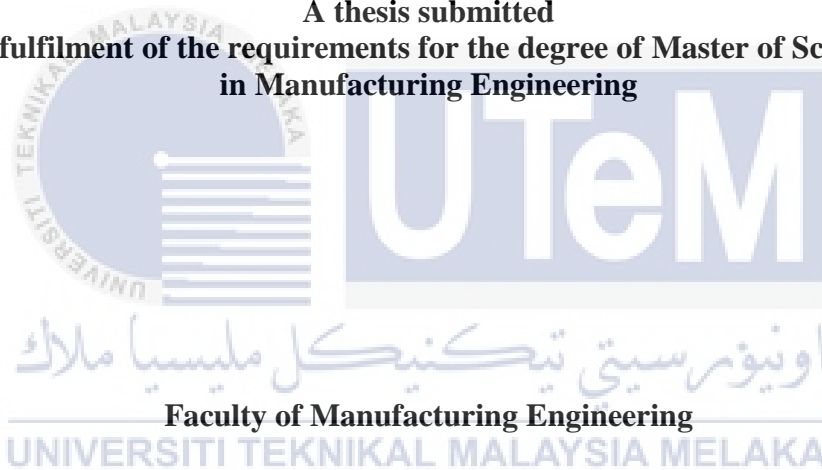
Master of Science in Manufacturing Engineering

2021

**INFLUENCE OF SOL AND DEPOSITION METHOD IN
DEVELOPING TiO₂ BROOKITE COATINGS**

FARAH HANUM BINTI SUZAIM

**A thesis submitted
in fulfilment of the requirements for the degree of Master of Science
in Manufacturing Engineering**





UNIVERSITI TEKNIKAL MALAYSIA MELAKA

2021

DECLARATION

I declare that this thesis entitled “Influence of Sol and Deposition Method in Developing Sol-Gel in TiO₂ Brookite Coatings” is the result of my own research except as cited in the references. The thesis has not been accepted for any degree and is not concurrently submitted in candidature of any other degree.



Signature :

Name :

Date :

اوتيمور سيتي تیکنیکل ملیسيا ملاک

UNIVERSITI TEKNIKAL MALAYSIA MELAKA

APPROVAL

I hereby declare that I have read this thesis and in my opinion this thesis is sufficient in terms of scope and quality for the award of Master of Science in Manufacturing Engineering.

Signature	:
Supervisor Name	:
Date	:



اونيورسيتي تيكنيكل مليسيا ملاك
UNIVERSITI TEKNIKAL MALAYSIA MELAKA

DEDICATION

To my beloved family



ABSTRACT

Brookite is highly promising photocatalyst due to its high photoactivity performance and significant hydrophilic ability. However, the development and application of pure sol-gel brookite coating is less reported. Therefore, the main objective of this research is to deposit brookite TiO_2 sol-gel coatings derived from 'green formulated sol' for self-cleaning application. The TiO_2 coatings were fabricated from various hydrolysis ratio, temperatures and deposition method. The hydrolysis ratio of water to titanium (IV) isopropoxide (TTiP) used are 32:4 (W_{32}), 48:4 (W_{48}) and 64:4 (W_{64}). In this work, two deposition methods which are dip and spin coating are used to compare the influence of deposition methods on TiO_2 coating phase formation, particularly on identifying the brookite presence. The deposited TiO_2 coatings were then heated at various temperatures such as 200 °C, 300 °C, 400 °C and 500 °C and soaked for 3 hours. For phase analysis, X-ray diffraction (XRD) and Raman spectroscopy are used to examine the influence of sol and deposition method towards phase formation. The surface and cross sectional morphological of TiO_2 coating were analyzed by scanning electron microscope (SEM) observation. The crystallite size was calculated using Scherrer's equation. The optical and hydrophilic properties were conducted to examine the TiO_2 coating characteristic. Results show that the different sol formulations and deposition methods have an influence in brookite TiO_2 coating's development. XRD result indicate that a single peak emerged at 31.9° from spin method was referred to the (111) plane of brookite crystal. For the spin coating, Raman spectroscopy also indicate a dominant brookite characteristic (band at 322 cm^{-1} and 363 cm^{-1}). SEM analysis revealed that the spin coating produced a uniform coating compared to the dip coating. Besides, the surface coating of the deposited TiO_2 coating via dip coating showed cracks regardless of temperature used. The thickness of the TiO_2 coating via spin coating is thinner (447 nm) compared to the dip coating (887 nm). The crystallite size of the TiO_2 spin coating was larger (63.2 nm) compared to the crystallite size of the spin coated (18.7 nm). The band gap value of the TiO_2 spin coating was in the range of 3.32 eV - 3.46 eV (brookite characteristic) whereas for the TiO_2 dip coating, their band gap value was in the range of 3.05 eV - 3.18 eV (anatase characteristic). Furthermore, the TiO_2 spin coating exhibited more hydrophilic characteristic compared to the TiO_2 dip coating. For photoactivity performances, the brookite TiO_2 coating was found to be more effective in the degradation of methylene blue (90.65%) and photo-induced hydrophilicity (15.21°). As a conclusion, it is found that spin coating deposition with W_{64} sol formulation is preferable for brookite formation whereas dip coating is more suitable for anatase and rutile.

PENGARUH KAEDAH PEMENDAPAN DAN SOL DALAM PEMBENTUKAN SALUTAN TiO₂ BROOKITE

ABSTRAK

Brookite adalah fotokatalis yang sangat menarik kerana fotoaktiviti yang tinggi dan keupayaan hidrofilik yang ketara. Walau bagaimanapun, kemajuan dan aplikasi kepada brookite tulen salutan adalah kurang dilaporkan. Oleh itu, tujuan utama objektif kajian ini adalah untuk menghasilkan salutan brookite TiO₂ yang berasal dari 'sol larutan hijau' untuk aplikasi pembersihan diri. Salutan TiO₂ tersebut diperbuat daripada pelbagai nisbah hidrolisis, suhu dan kaedah pemendapan. Nisbah hidrolisis air ke TTP yang digunakan adalah 32:4(W₃₂), 48:4(W₄₈) dan 64:4(W₆₄). Dalam penyelidikan ini, dua kaedah pemendapan iaitu salutan celup dan putaran telah digunakan untuk membandingkan pengaruh kaedah pemendapan pada pembentukan fasa salutan TiO₂, terutamanya dalam mengenal pasti kehadiran brookite. Salutan TiO₂ dipanaskan pada pelbagai suhu seperti 200⁰C, 300⁰C, 400⁰C dan 500⁰C dan direhatkan selama 3 jam. Untuk analisis fasa, XRD dan spektroskopi Raman digunakan untuk mengkaji pengaruh sol dan proses pemendapan dalam pembentukan fasa. Salutan dan morfologi keratan rentas salutan TiO₂ dianalisis oleh pemerhatian SEM. Saiz kristal dihitung menggunakan persamaan Scherrer. Sifat optik dan hidrofilik dijalankan untuk mengkaji ciri-ciri salutan TiO₂. Keputusan menunjukkan bahawa formulasi sol dan kaedah pemendapan yang berbeza mempengaruhi dalam pembentukan salutan brookite TiO₂. Keputusan XRD dikaitkan dengan puncak tunggal pada 31.9° yang dirujuk kepada satah kristal brookite (111). Spektroskopi Raman juga menunjukkan ciri-ciri brookite (band pada 322 cm⁻¹ dan 363 cm⁻¹). Imej SEM dengan lebih lanjut mendedahkan bahawa TiO₂ yang disalut secara putaran menghasilkan salutan seragam berbanding TiO₂ yang disalut secara celupan. Sementara itu, imej SEM permukaan salutan TiO₂ melalui salutan celupan menunjukkan salutan retak tanpa mengira sebarang suhu. Selain itu, ketebalan salutan TiO₂ salutan melalui salutan putaran adalah lebih nipis berbanding ketebalan salutan celup TiO₂ dengan 447 nm dan 887 nm. Saiz kristal TiO₂ yang disalut secara putaran adalah lebih besar (63.2 nm) berbanding saiz kristal TiO₂ yang disalut secara celupan (18.7 nm). Nilai jurang band TiO₂ disalut secara putaran didapati dalam lingkungan 3.32 eV - 3.46 eV (ciri-ciri brookite) manakala bagi TiO₂ disalut secara celupan, nilai jurang band didapati dalam lingkungan 3.05 eV – 3.18 eV (ciri-ciri anatase). Tambahan lagi, TiO₂ yang disalut secara proses putaran menunjukkan sifat hidrofilik yang lebih tinggi berbanding TiO₂ yang disalut secara celupan. Untuk keupayaan fotoaktiviti, salutan brookite TiO₂ didapati lebih berkesan dalam penurunan kadar metil biru (90.65%) dan fotoinduksi hidrofilik (15.21⁰). Sebagai kesimpulan, didapati proses pemendapan salutan putaran dengan formulasi sol W₆₄ adalah lebih baik untuk pembentukan brookite manakala salutan celupan lebih sesuai untuk anatase dan rutil.

ACKNOWLEDGEMENTS

Alhamdulillah, all praises and thanks to Allah, for His blessing and allowing me to finish this thesis with all the hurdles and challenge that I have to go through. Special appreciation goes to my supervisor, Associate Professor Ts. Dr. Zulkifli Bin Mohd Rosli for his supervision and constant support. His invaluable help of constructive comments and suggestions throughout the experimental and thesis works have contributed to the success of this research. It has been a great pleasure and honour to have him as my supervisor. Not forgotten my appreciation to my co-supervisor, Associate Professor Ts. Dr. Umar Al-Amani Bin Haji Azlan for his support and knowledge regarding the topic. My sincere thanks also goes to Associate Professor Dr. Jariah Binti Muhamad Juoi for her support and help towards my postgraduates affairs.

Special thanks to the financial support given by the Ministry of Higher Education Malaysia and Universiti Teknikal Malaysia Melaka (UTeM) through fundamental grant. My acknowledgement also goes to all the technicians and office staffs of Faculty of Manufacturing Engineering for their co-operations. Sincere thanks are extended to all my friends for their kindness and moral support during my study. Thanks for the friendship and memories.

Last but not least, my deepest gratitude to my beloved parents, Suzaim bin Parman and Norzalina binti Ibrahim, I owe you everything that I am, that I have been, and I will be. Thank you for believing in me and understanding my struggles. Also not forgetting my brothers, Faris Haziq and Farhan Hadi for their endless love and care. I love you all.

TABLE OF CONTENTS

	PAGE
DECLARATION	
APPROVAL	
DEDICATION	
ABSTRACT	i
ABSTRAK	ii
ACKNOWLEDGEMENTS	iii
TABLE OF CONTENTS	iv
LIST OF TABLES	vii
LIST OF FIGURES	viii
LIST OF APPENDICES	xiii
LIST OF ABBREVIATIONS	xiv
LIST OF SYMBOLS	xv
LIST OF PUBLICATIONS	xvi
CHAPTER	
1. INTRODUCTION	1
1.1 Background of study	1
1.2 Problem statement	4
1.3 Research questions	7
1.4 Research objectives	7
1.5 Research scopes	7
1.6 Thesis structure	8
1.7 Summary	9
2. LITERATURE REVIEW	10
2.1 Introduction	10
2.2 Titanium dioxide	10
2.2.1 Properties of TiO ₂	11
2.3 Coating thin film technique	13
2.3.1 Chemical vapor deposition (CVD)	14
2.3.2 Physical vapor deposition (PVD)	15
2.3.3 Sol-gel method	16
2.4 Sol-gel derived coating technique	21
2.4.1 Dip-coating	21
2.4.2 Spin coating	23
2.4.3 Spray coating	25
2.5 Brookite	26
2.5.1 Brookite preparation	26
2.5.2 Brookite characterization	28
2.5.3 Optical band gap of brookite	33
2.5.4 Hydrophilic property of brookite	34
2.6 Photocatalytic mechanism	37

2.7	Photoinduced hydrophilicity mechanism	40
2.8	Application of brookite hydrophilic surface	42
2.9	Summary	44
3.	RESEARCH METHODOLOGY	46
3.1	Introduction	46
3.2	Flow chart of the experiment	47
3.3	Material and specification	48
3.4	List of apparatus	48
3.5	Phase characterization on TiO ₂ coating glass substrate	49
3.5.1	X-ray diffraction (XRD)	49
3.5.2	Raman spectroscopy	50
3.6	Morphology and thickness analysis by Scanning Electron Microscopy (SEM)	50
3.7	Optical property by UV-Vis spectrophotometer	51
3.8	Hydrophilic property by water contact angle measurement	51
3.9	Photocatalytic activity measurement	52
3.10	Phase 1: Synthesizing of TiO ₂ coating	53
3.10.1	Preparation of TiO ₂ solution	53
3.10.2	Deposition of TiO ₂ solution	55
3.11	Phase 2: Morphological, optical characterization and hydrophilic properties on TiO ₂ coating	59
3.12	Phase 3: Photoactivity measurement on anatase TiO ₂ dip coating and brookite TiO ₂ spin coating	59
3.13	Summary	60
4.	RESULTS AND DISCUSSION	62
4.1	Introduction	62
4.2	Influence of sol and deposition method towards coating phases	62
4.2.1	The XRD and Raman of the dip coating	62
4.2.2	XRD and Raman of the spin coating	67
4.2.3	Phases comparison via dip coating and spin coating at various temperatures	71
4.3	Comparison on the characteristics and properties of the W ₆₄ coatings deposited via dip and spin method	72
4.3.1	Surface morphology	73
4.3.2	Coating thickness	75
4.3.3	Crystallite size	78
4.3.4	Optical property	80
4.3.5	Hydrophilicity property	82
4.4	Comparison on the photoactivity performance	85
4.4.1	The photocatalytic performance of the brookite and the anatase coating	85
4.4.2	Photo induced hydrophilicity performance of the brookite and the anatase coating	91
4.5	Summary	93
5.	CONCLUSION AND RECOMMENDATIONS	95
5.1	Conclusion	95

5.2 Recommendations	96
REFERENCES	98
APPENDICES	118



LIST OF TABLES

TABLE	TITLE	PAGE
2.1	Physical and chemical properties of the TiO ₂ structures (Yu et al., 2018)	13
2.2	Sol-gel derived coating techniques and their working principle (Tyona, 2013; Luangkularb et al., 2014; Varela et al., 2017)	21
2.3	Literature on the band gaps of rutile, anatase, and brookite	34
2.4	Relationship of contact angle values and wettability (Marmur et al., 2017)	36
3.1	List of material	48
3.2	Different hydrolysis formulation of TiO ₂ solution used	54
4.1	Thickness of TiO ₂ coating via dip coating	77
4.2	Thickness of TiO ₂ coating via spin coating	77
4.3	Crystallite size of TiO ₂ (W ₆₄) deposited via dip method	79
4.4	Crystallite size of TiO ₂ (W ₆₄) deposited via spin method	79
4.5	Absorbance of methylene blue standard	87
4.6	Methylene blue degradation of anatase and brookite TiO ₂ coating after exposing to UV high irradiation	89
4.7	Dependence of photo-induced change in CA of anatase and brookite TiO ₂ coating after exposin to UV light irradiation	93

LIST OF FIGURES

FIGURE	TITLE	PAGE
1.1	Main areas of TiO ₂ photocatalysis (Nakata and Fujishima, 2012)	4
2.1	Crystal structure of TiO ₂ (Haggerty et al., 2017)	12
2.2	Schematic diagram for chemical vapor deposition (CVD) (Zhang et al., 2016)	15
2.3	Schematic diagram for physical vapor deposition (CVD) (Wang et al., 2014)	16
2.4	Schematic diagram for sol-gel method (Rao et al., 2017)	17
2.5	Stages in sol-gel process (Brinker and Scherer, 2013)	18
2.6	Polymerization of partially hydrolyzed molecules (Danks et al., 2016)	19
2.7	Diagram of sol and gel (Maleki et al., 2014)	20
2.8	Dip-coating process (Varela et al., 2017)	23
2.9	Spin-coating process (Tyona, 2013)	24
2.10	Spray coating process (Zabihi et al., 2015)	26
2.11	Representative octahedron of the crystalline structure of brookite (Samat et al., 2016)	29
2.12	X-ray diffraction (XRD) analysis patterns of brookite sol-gel spin coated heated at 400°C (Komariah et al., 2016)	31

2.13	Raman spectra of brookite (Iliev et al., 2013)	32
2.14	SEM morphology of brookite TiO ₂ heated at 400°C (Komariah et al., 2016)	33
2.15	Type of contact angle for (a) hydrophobic and (b) hydrophilic surface (Baltatu et al., 2018)	35
2.16	The schematic of TiO ₂ photocatalytic mechanism (Samsudin et al., 2015)	38
2.17	The progress of photo-induced hydrophilicity (a) 0s (b) 15s (c) 30s (d) 45s and (e) 75s by UV light irradiation (Zhange et al., 2012)	41
3.1	Schematic flow chart of the experiment	47
3.2	Step of TiO ₂ coating preparation	53
3.3	Sequence for the preparation of TiO ₂ solution	54
3.4	Step of TiO ₂ coating deposition on glass substrates	55
3.5	Step of TiO ₂ cleaning glass substrate	56
3.6	TiO ₂ deposition using dip-coating	57
3.7	TiO ₂ deposition using spin-coating	57
3.8	The heating profile for TiO ₂ coating	58
4.1	The XRD patterns for the W ₃₂ for dip coating	63
4.2	The XRD patterns for the W ₄₈ for dip coating	64
4.3	The XRD patterns for the W ₆₄ for dip coating	64
4.4	The Raman Spectra of W ₃₂ for dip coating	65
4.5	The Raman Spectra of W ₄₈ for dip coating	66
4.6	The Raman Spectra of W ₆₄ for dip coating	66

4.7	The XRD patterns for the W ₃₂ for spin coating	67
4.8	The XRD patterns for the W ₄₈ for spin coating	68
4.9	The XRD patterns for the W ₆₄ for spin coating	68
4.10	The Raman Spectra of W ₃₂ for spin coating	69
4.11	The Raman Spectra of W ₄₈ for spin coating	70
4.12	The Raman Spectra of W ₆₄ for spin coating	70
4.13	The XRD pattern of the deposited TiO ₂ coatings as compared to powder coating annealed at 400°C. (Note that, the powder obtained was from the same formulation of W ₆₄ by heating the TiO ₂ sol at 400°C with 3 hours of soaking time)	72
4.14	SEM Micrograph of glass substrate without coating	73
4.15	SEM surface morphologies of the TiO ₂ coating deposited via dip coating at various temperature (a) 200°C (b) 300°C (c) 400°C, and (d) 500°C	74
4.16	SEM surface morphologies of the TiO ₂ coating deposited via spin coating at various temperature (a) 200°C (b) 300°C (c) 400°C, and (d) 500°C	75
4.17	SEM cross sectional morphologies of the TiO ₂ coating deposited via dip coating at various temperature (a) 200°C (b) 300°C (c) 400°C, and (d) 500°C	76
4.18	SEM cross sectional morphologies of the TiO ₂ coating deposited via spin coating at various temperature (a) 200°C (b) 300°C (c) 400°C, and (d) 500°C	77

4.19	The average value of SEM cross sectional morphologies of the TiO ₂ coating deposited via dip and spin coating	78
4.20	Crystallite size of the TiO ₂ coating deposited via dip and spin method	79
4.21	The optical band gap of the TiO ₂ coating deposited via dip coating at various temperature (a) 200°C (b) 300°C (c) 400°C, and (d) 500°C	81
4.22	The optical band gap of the TiO ₂ coating deposited via spin coating at various temperature (a) 200°C (b) 300°C (c) 400°C, and (d) 500°C	82
4.23	Contact angle measurement of TiO ₂ coating via dip method at various temperature (a) 200°C (b) 300°C (c) 400°C, and (d) 500°C	84
4.24	Contact angle measurement of TiO ₂ coating via spin coating at various temperature (a) 200°C (b) 300°C (c) 400°C, and (d) 500°C	84
4.25	The absorbance spectra of the brookite and anatase coating	86
4.26	Absorption spectra of methylene blue standards: 0.1ppm, 0.15ppm, 0.2ppm, 0.25ppm, and 0.3ppm	86
4.27	Percentage of methylene blue degradation of the deposited brookite and anatase TiO ₂ coating at 400°C	88
4.28	Photocatalytic of anatase and brookite TiO ₂ coating of methylene blue under UV light	90
4.29	MB Degradation for the anatase coating	90

4.30	MB Degradation for the brookite coating	91
4.31	CA of anatase and brookite TiO ₂ coating under UV light irradiation	92



LIST OF APPENDICES

APPENDIX	TITLE	PAGE
A	JCDPS No of Anatase	118
B	JCDPS No of Brookite	121
C	JCDPS No of Rutile	126

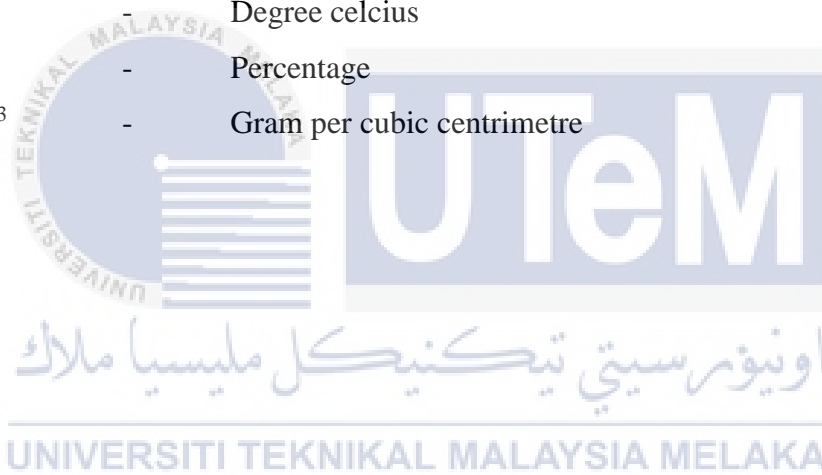


LIST OF ABBREVIATIONS

AOPs	-	Advanced Oxidation Processes
CA	-	Contact angle
CeO ₂	-	Cerium Oxide
CVD	-	Chemical Vapor Deposition
EDX	-	Energy Dispersive X-Ray
H ₂ O	-	Water
HCl	-	Hydrochloric Acid
MB	-	Methylene Blue
OH	-	Hydroxyl
SnO ₂	-	Tin Oxide
PVD	-	Physical Vapor Deposition
SEM	-	Scanning Electron Microscopy
TiO ₂	-	Titanium Dioxide
TTiP	-	Titanium (IV) Isopropoxide
UV Vis	-	Ultraviolet Visible
WO ₃	-	Tungsten Trioxide
XRD	-	X-Ray Powder Diffraction
ZnO	-	Zinc Oxide
ZnS	-	Zinc Sulfide

LIST OF SYMBOLS

e	-	Electron
λ	-	Wavelength
eV	-	Energy Gap
cm	-	Centimeter
nm	-	Nanometer
h	-	Hour
°C	-	Degree celcius
%	-	Percentage
g/cm ³	-	Gram per cubic centrimetre



LIST OF PUBLICATIONS

Suzaim, F. H., Rosli, Z. M., and Juoi, J. M., T. Moriga, 2019. Effect of heating temperature on brookite TiO₂ sol-gel coating for photo-induced hydrophilicity. Accepted for publication in *Journal of Advanced Manufacturing Technology*.

Suzaim, F. H., Rosli, Z. M., and Juoi, J. M., 2018. Influence of water volume and heating temperatures on type of phases and crystallite size of sol-gel thin films deposited without solvent. *International Journal of Engineering & Technology*, 7(4), pp. 5067–5071.



CHAPTER 1

INTRODUCTION

1.1 Background of study

Since the encounter of the prevalent waste water treatment, compelling methods to degrade organic pollutants and microorganisms has been widely explored to provide fresh and clean water. Advanced Oxidation Processes (AOPs) methods agree upon a better environmental technological approach to produce the potential for excellent removal of organic pollutant and microorganisms in order to deal with increasing wastewater problem and develop cost-effective to societies (Bhattacharya et al., 2013). Furthermore, the present of recent advanced technology in modern economy and society requires good technical efficiency, low cost and various nanostructure for removal treatment process (Savage et al., 2005; Samantha et al., 2016).

There is some of the renewable energy technologies are applied to treat wastewater in the long term period such as bio-fuel, solar energy, biomass and wind power. In particular, AOPs is being used as water purification due to its ability in absorbing energy, high efficiency and becoming more critical to eliminate pollutants in wastewater. It is imperative that the increase of energy during AOPs reaction is sought after as the effectiveness of performance is measured by these conditions (Martin et al., 2011; Taknabe et al., 2017).

Among the available AOPs, the development of heterogenous photocatalysis has performed as the most favourable for the approaching wastewater experiment. In the recent decade, heterogenous photocatalysis has been widely studied which used solid catalyst under light irradiation (UV and visible light) to totally degrade organic pollutant and microorganisms present in water. Moreover, some potentially semiconductor metal oxide

materials with enough sufficient band gap energy like titanium dioxide (TiO_2), cerium oxide (CeO_2), zinc oxide (ZnO) as well as tin oxide (SnO_2) are mainly acting as heterogenous photocatalysts and being used in photocatalytic application (Ibhadon and Fitzpatrick 2013; Byrne et al., 2015; Hodges et al., 2018). The present of available semiconductor catalyst such as low wavelength absorption, instability for catalysis, toxicity and low recombination rate have constrained the performance of the photocatalytic reaction. With these limitations, there is a need to circumvent the issue in order to improve high performance of photocatalytic reaction with greater rate of light absorption and longer lifecycle of catalyst (Rochkind et al., 2015).

To date, TiO_2 is is the most suitable being used as semiconductor photocatalyst due to the excitation of the semiconductor catalyst under UV light irradiation (Lu et al., 2011; Leong et al., 2014; Tsang et al., 2019). The efficiency of the TiO_2 photocatalytic properties is depended on the particle size, crystallinity, surface area, crystallite phase and composition, porosity, band gap, surface defects and the density of surface hydroxyl (Yasmina et al., 2014; Pawar et al., 2018). Another property that can be measured by exposing TiO_2 surface under UV light is its hydrophilicity which is known as photoinduced hydrophilicity (Zhang et al., 2012). Photo-induced hydrophilicity phenomenon is a mechanism when the formation of the hydroxyl group with TiO_2 surface interacts with the presence of UV light (Machida et al., 2018). Theoretically, photoinduced hydrophilicity efficiency increases as the hydroxyl group (OH^-) increases (Jun et al., 2015a). The more interface of the hydroxyl group along the TiO_2 surface, the more the water droplet will spread out onto the surface. Thus, the mutual action between the hydrophilicity and the photocatalytic activities will reinforce each other and can be used as a self-cleaning application (Guan et al., 2005).

In comparison with TiO₂ powder, the TiO₂ coating does not form conglomeration and provide high surface activity, allowing the material use in wide industrial applications including self-cleaning and anti-bacterial (Chen et al., 2009). TiO₂ coating can be prepared through numerous procedures such as sol-gel method, hydrolysis deposition, chemical vapor deposition, electrodeposition and chemical spray pyrolysis. Among the many techniques, sol gel method is considered the most suitable to be used due to its ability to provide excellent homogeneity and easy on controlling the particle size and morphology (Alzamani et al., 2013; Danks et al., 2016; Liang et al., 2018). Thus, in order to deposit TiO₂ coating on glass substrate, a dip and spin-coating technique are going to be used in this study. Dip and spin coating method is commonly adopted for depositing TiO₂ on glass substrate because it easy to conduct and has advantage to control the thickness of TiO₂ coating.

Thus, the application of TiO₂ is attractive for many reason. TiO₂ has been intensively used in photocatalytic activities, photoinduced hydrophilicity (for example self cleaning glass), solar cells, optoelectronic applications and gas sensors. In recent decade, TiO₂ photocatalysis become more attractive and considered as the most promising semiconductor for purification of water and air (Liu et al., 2006; Nakamura et al., 2010). Moreover, the TiO₂ photocatalyst and hydrophilic properties can react concurrently on the same surface even if the reaction is entirely different (Banerjee et al., 2015). The formation of water droplet on the TiO₂ coating surface and the photocatalytic degradation of organic pollutants resulted in self-cleaning effect. Recently, the researchers began to pay attention to the development of self-cleaning material due to its wide applications in view of environment, indoor application, solar panel and building material. Figure 1.1 displays the main area of TiO₂ depending on its photocatalysis activity.